# Fluoride Ion Sensing and Caging by a Preformed Molecular D4R Zinc Phosphate Heterocubane

Alok Ch. Kalita and Ramaswamy Murugavel*

Department of Chemistry, Indian Institute of Technology-Bombay, Powai, Mumbai-400076, India

S *Supporting Information*

ABSTRACT: Double-4-ring (D4R) zinc phosphate $[Zn(dipp)(DMSO)]_4$ (**1**, dipp = 2,6-di-*iso*-propylphenylphosphate, DMSO = dimethyl sulfoxide), on treatment with a free fluoride ion source, exhibited ability to sense and capture fluoride ions from a variety of sources, as evidenced by extensive solution ^{31}P and ^{19}F NMR spectral titration studies. The fluoride ion-encapsulated cage $[^nBu_4N][F@\{Zn(dipp)(DMSO)\}_4]$ (**2**) was isolated in good yield from an equimolar reaction between **1** and $^nBu_4NF$ in methanol and characterized by analytical and spectroscopic methods. When 1-methyl-4,4′-bipyridin-1-ium fluoride (MeQ-F) was used as the fluoride ion source a zwitterionic cage $[F@\{Zn_4(dipp)_4(MeQ)(DMSO)_3\}]$ (**3**) was isolated. Crystal structure determination for **3** confirmed not only fluoride incorporation inside the D4R cage but also a weak interaction of the central fluoride ion with all four zinc centers of the cubane, resulting in a trigonal bipyramidal geometry around the zinc centers. To establish the selectivity, cubane **1** was treated with 2 equiv of MeQ-X (X = various anions) under similar conditions to isolate $[F@\{Zn_4(dipp)_4(MeQ)_2(MeOH)_2\}][X]$ (X = I **4**; BF_4 **5**; PF_6 **6**) in good yields. The crystal structure determination of **4** and **5** showed that the iodide and tetrafluoroborate anions are found outside the cage while fluoride ion has entered the cavity. The final fluoride encapsulated D4R cage is anionic in **2**, neutral in **3**, and cationic in **4−6**, showing the versatility of the cubane framework to stabilize fluoride ions in all three forms. NMR titrations showed that **1** can sense even 1 ppm level of fluoride ions and sequester them from fluoridated water and toothpaste extract.
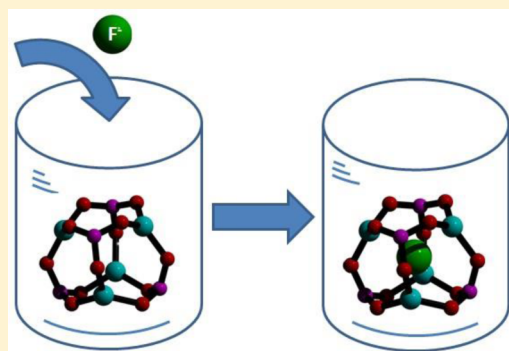
INTRODUCTION

Chemical sensing and scavenging are two rigorously investigated areas in recent times due to environmental and security concerns.[1,2] In particular, development of reliable sensors for anions such as F^-, NO_3^-, SO_4^{2-}, and PO_4^{3-} inside suitably designed molecular pockets, cages, and clathrates has been an active area of research.[3] Among various anions, fluoride ion sensing is of specific interest owing to the high toxicity of soluble fluorides. Soluble fluorides are commonly found beyond a certain level in domestic products such as toothpaste (Na_2PO_3F), dietary supplements (NaF), glass-etching or chrome-cleaning agents (NH_4HF_2), insecticides, rodenticides (NaF), and also in drinking water (NaF). The lethal dose for adults is 32−64 mg of elemental fluoride per kilogram of body weight. The dose that leads to adverse health effects such as crippling skeletal fluorosis is often roughly about one-fifth of the lethal dose.[4,5] In most cases fluoride poisoning is caused by drinking water containing more than 2−3 ppm levels of fluoride.[5]

Colorimetry and electrochemistry (ion selective electrodes) have been utilized to measure the extent of fluoride sensing in many instances.[6] An alternative strategy, to not only sense but also sequester fluoride ions from solution, is to make use of the empty space available within the preformed inorganic cages. Encapsulation of small molecules and ions inside the cluster cavities during the cage/cluster formation phase been demonstrated recently in a few instances.[7−9] As a specific example, molecular clusters possessing D4R core structure have been employed to encapsulate atomic species through the isolation of hydrogen-encapsulated T8 cages by γ-irradiation of octasilsesquioxanes.[7]

Bassindale et al. have isolated fluoride ion-encapsulated T8 silsesquioxane cages by carrying out the hydrolysis of trialkoxy silanes in the presence of a fluoride source.[8,9] In a typical synthesis, $RSi(OEt)_3$ is hydrolyzed in chloroform in the presence of tetrabutylammonium fluoride $(^nBu_4NF)$ (**1**).[8] This reaction also works well with germanium to produce fluoride-encapsulated germanium T8 clusters $[RGeO_{1.5}]_8$.[10] Encapsulation of fluoride ion inside a D4R vanadium phosphate during the cluster formation has also been reported.[11] Similarly, the chemistry of framework solids that has been developing over the last two decades has seen an increased number of instances where fluoride ions get incorporated inside the framework cages during the synthesis of such frameworks, which often leads to enhanced stability of the framework solids.[12,13]

$$[RSi(OEt)_3] \xrightarrow[CHCl_3]{^nBu_4NF} F@[RSiO_{1.5}]_8 \qquad (1)$$
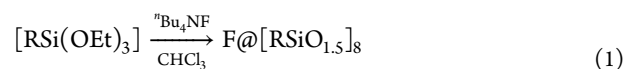
All the above-mentioned examples of fluoride incorporation take place during the cage formation or synthesis phase, and to our knowledge there have been no instances in the published literature where a preformed inorganic molecular cage has been shown to be a selective fluoride sensor. Our recent success in synthesizing a large variety of organic-soluble cage-like molecular phosphates[14] and phosphonates[15] provided us an opportunity to investigate the possibility of using small preformed D4R zinc phosphates to sense, complex, and capture fluoride ions.

Methanol-soluble D4R phosphate $[Zn(dipp)(DMSO)]_4$ (**1**) (dipp = di-*iso*-propylphenylphosphate) (Figure 1), which can
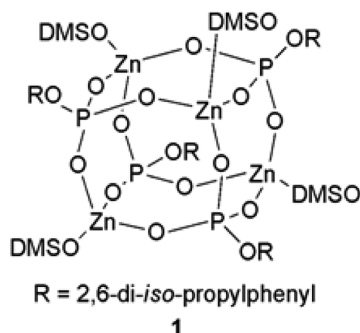

Figure 1. Structure of D4R cubane with labile DMSO ligands.

be synthesized in quantitative yield from inexpensive starting materials such as zinc acetate and a phosphoric acid monoester, was employed as the host in the present study to sense and cage fluoride ions. The architecture of cage molecule **1** is such that the DMSO ligands on the zinc centers point away from the cubane and hence do not block the access to the cavity.

■ RESULTS AND DISCUSSION

NMR Titrations Involving $[Zn(dipp)(DMSO)]_4$ (1). Cluster **1** dissolved in CD_3OD exhibits a single sharp resonance in the ^{31}P NMR spectrum at −4.2 ppm, owing to the highly symmetric nature of the cluster. It can be envisaged that when fluoride ion enters the cage, it would be somewhat proximal to the phosphorus centers and hence should result in a significant shift of the phosphorus resonance. Hence, to probe the ability of **1** to encapsulate fluoride ions, ^{31}P NMR spectral titrations were employed (Figure 2). Spectrum a depicts the observed spectrum of a CD_3OD solution of **1** (1×10^{-5} M) before addition of F^- ions. It can be seen from spectrum b that the addition of 1×10^{-6} M of $^nBu_4NF$ produces a new signal at 3.2 ppm, which is roughly 7 ppm downfield-shifted relative to the signal for pure **1**. Successive quantities of $^nBu_4NF$ added to this solution increase the intensity of the 3.2 ppm signal to the same extent as the decrease in intensity of the signal at −4.2 ppm. After addition of 1.0×10^{-5} M $^nBu_4NF$, the signal at −4.2 ppm completely disappears (spectrum d in Figure 2). These studies thus provide evidence for a change in the structure of **1** that affects equally the chemical shift of all four phosphorus atoms of the D4R structure, which is possible only if the fluoride ion enters the cubane and occupies the empty space available at the center of the cubane. Since the center of the cubane to the phosphorus atoms is much longer for any bonding interactions, only a weak interaction of the fluoride ion with the four phosphorus atoms is expected, leading to a small shift in the ^{31}P NMR signal. Similar titrations carried out with other halides
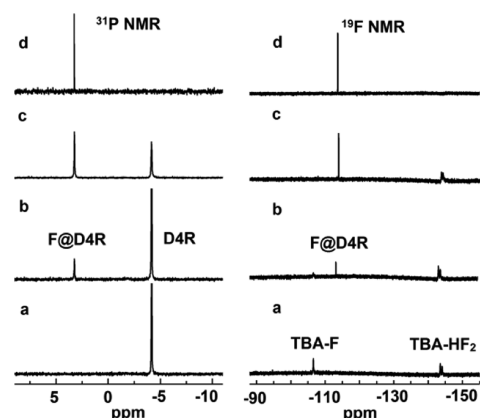

Figure 2. (left) The ^{31}P NMR spectral titration (CD_3OD) of a 1×10^{-5} M solution of **1** with the following concentrations of $^nBu_4NF$: (a) none; (b) 1×10^{-6} M; (c) 5×10^{-6} M; (d) 1×10^{-5} M. (right) The ^{19}F NMR spectrum (CD_3OD) of a 5×10^{-6} M solution of $^nBu_4NF$ with the following concentrations of **1**: (a) none; (b) 2×10^{-6} M; (c) 3×10^{-6} M; (d) 5×10^{-6} M.

(Cl^-, Br^-, and I^-) did not result in any change in the observed ^{31}P NMR spectrum, indicating the selectivity of **1** toward only fluoride sensing.

A reverse titration was performed to track the movement of fluoride ions from $^nBu_4NF$ ($\delta_F = -106$ ppm; Figure 2, right) to the center of the cubane. Addition of 1 equiv of **1**, in several steps, leads to the complete disappearance of the −106 ppm signal, with a new resonance appearing at −113 ppm, supporting the ^{31}P NMR studies and also confirming incorporation of fluoride ion inside the cubane (Figure 2, spectrum d).

Synthesis and Spectra of Compounds 2 and 3. To isolate the fluoride-incorporated cubane, a methanol/DMSO solution of **1**, freshly prepared from the reaction of $Zn(OAc)_2 \cdot 2H_2O$ with dipp-H_2, was treated with $^nBu_4NF$ at ambient conditions. $[^nBu_4N][F@\{Zn(dipp)(DMSO)\}_4]$ (**2**) (Scheme 1) was isolated as the only product and characterized by analytical and spectroscopic measurements (Supporting Information, Figure S1 and Table S1).

Scheme 1. Synthesis of 2
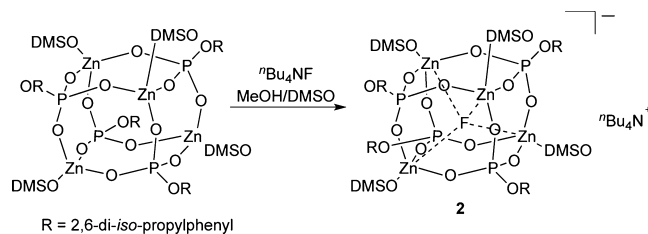
The Fourier transform infrared (FT-IR) spectrum exhibits strong absorptions at 1147, 1037, and 908 cm^{-1} for characteristic P=O stretching and M−O−P asymmetric and symmetric stretching vibrations, respectively (Figure 3).[14] The ^1H NMR spectrum shows well-separated resonances for the protons of the di-*iso*-propylphenyl group and tetrabutylammonium cation in a 4:1 ratio. Isopropyl −CH and −CH_3 groups exhibit a septet and a doublet at 3.8 and 1.08 ppm, respectively. As was observed during the ^{31}P NMR titration studies (vide supra), the ^{31}P NMR spectrum of the isolated product exhibits a singlet at 2.5 ppm in DMSO-d_6. A single resonance at −113

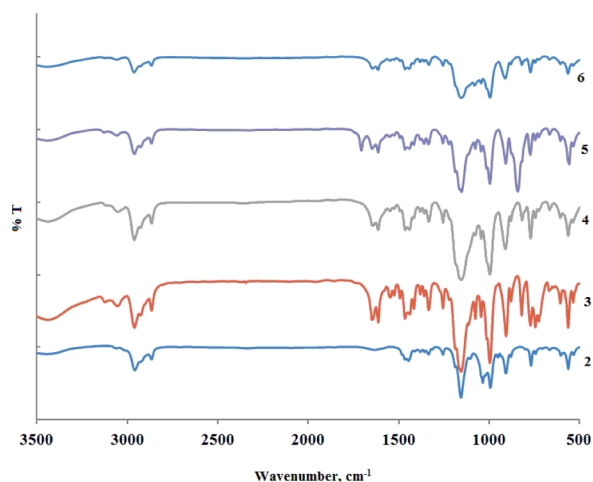**Figure 3.** FT-IR spectra of compounds **2**−**6** diluted in KBr disc.

ppm in ^{19}F NMR spectrum is also consistent with the ^{19}F NMR titration studies described above.

Additional evidence for the fluoride incorporation comes from negative ion electrospray ionization (ESI) mass spectral (MS) studies, which produce MS peaks under mild ionization conditions with the expected isotopic distribution for [**2**-4DMSO]$^{−}$, [**2**-3DMSO]$^{−}$, and [**2**-2DMSO]$^{−}$ ions. The MS depicted in Figure 4 confirms the fluoride incorporation
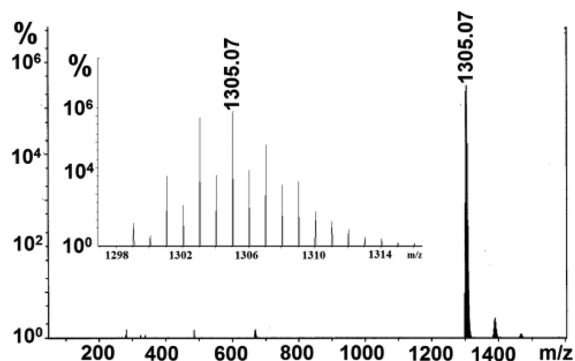

Figure 4. Negative ion ESI MS of compound **2**.

through the peak appearing at m/z 1305.07, corresponding to [F@{Zn(dipp)}$_4$]$^{−}$ ion. The host cluster **1** produces a signal at m/z 1543.03 with the isotopic distribution that corresponds to [**1**-DMSO+Na]$^{+}$ ion in ESI MS (positive ion mode) (Supporting Information, Figure S2).

While it has been clearly established by a combination of analytical and spectroscopic studies that compound **2** represents the fluoride ion-incorporated version of **1**, all attempts to obtain single crystals of **2** have been unsuccessful, presumably due to the disorder-prone tetrabutylammonium countercation. Hence the synthetic strategy was modified by choosing *N*-methylviologen hexafluoroantimonate, [MeQ]-SbF$_6$, as fluoride ion source, which can also act as a pyridinic ligand for the cage zinc ions. The pyridinic part of the MeQ cation can be expected to replace a DMSO on one of the zinc centers on the cubane to produce a cationic cubane, which can then cage the fluoride ion to produce an anion-incorporated cationic cage. As anticipated, treatment of **1** with [MeQ]SbF$_6$ proceeds smoothly under similar reaction conditions to yield [F@{Zn$_4$(dipp)$_4$(DMSO)$_3$(MeQ)] (**3**) as single crystals. The

^{1}H and ^{31}P NMR spectral characteristics of **3** are very similar to **2** (Supporting Information, Table S1, Figure S4). A single resonance at $\delta = -113$ ppm is observed in the ^{19}F NMR spectrum for the encapsulated fluoride in **3** as in the case of **2**.

Molecular Structure of Compound 3. Single-crystal structure analysis reveals that compound **3** crystallizes in the orthorhombic noncentrosymmetric $P2_12_12_1$ space group. The asymmetric unit of **3** is featured by the Zn$_4$P$_4$O$_{16}$ D4R core as in the case of parent cubane **1**, albeit with two major differences (Figure 5). The first is the presence of fluoride ion at the center
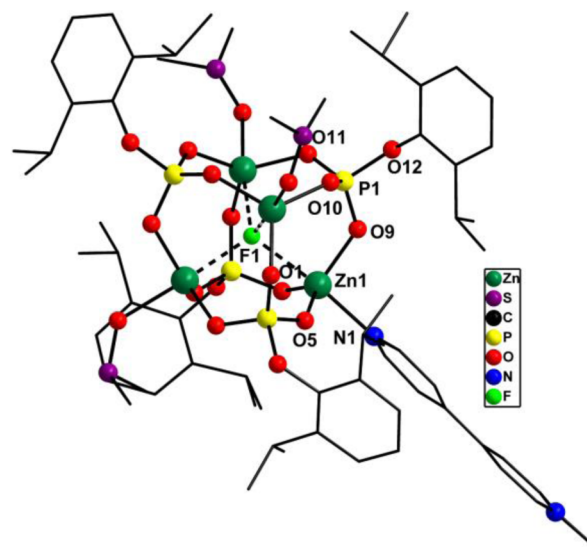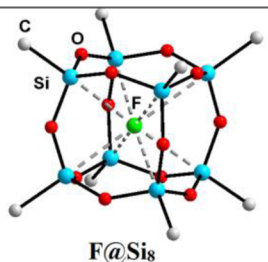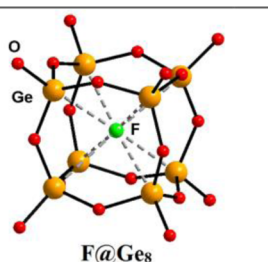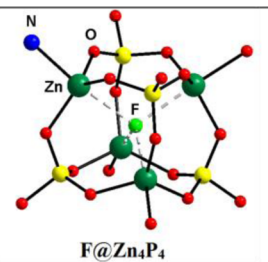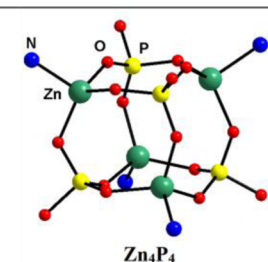

Figure 5. Molecular structure of **3**. Selected bond distances [Å]: Zn−O 1.911(3)−1.948(3) (av 1.928), P−O(Zn) 1.497(3)−1.527(3) (av 1.507), P−O(Ar) 1.606(3)−1.619(3) (av 1.614), Zn−F 2.224(2)−2.447(2) (av 2.332), P−F 2.910(2)−2.967(2) (av 2.939); bond angles [deg]: O−Zn−O (equatorial) 116.12(2)−124.94(1) (av119.32), O−Zn−O (axial) 89.57(1)−93.80(1) (av 91.59), N−Zn−O 88.30(1)−98.13(2) (av 94.75), O−Zn−F 80.93(1)−88.10(1) (av 85.31), ∠P 103.40(2)−115.21(2) (av 109.22), Zn−O−P 122.47(2)−134.9 (2) (av127.31).

of cubane, showing significant but weak interactions with all four zinc centers. The second difference is the change in coordination geometry around the tetrahedral zinc centers in Zn$_4$P$_4$ cubanes to distorted trigonal bipyramidal (tbp) in **3** (Figure 5).

Since the MeQ$^+$ ion binds only to one of the four zinc centers of the cubane, two types of Zn centers are found. Three of the four zinc centers are surrounded by three phosphate oxygen atoms at the equatorial positions (av Zn−O 1.928 Å), one DMSO oxygen at one of the axial positions, and the weakly bound fluoride ion in the other axial position (av Zn···F 2.332 Å). The fourth and the unique zinc atom is coordinated to three phosphate oxygen atoms (the Zn(1)−O(9) 1.913(3), Zn(1)−O(5) 1.923(3), and Zn(1)−O(1) 1.915(3) Å unit) at the equatorial plane, one axial pyridyl nitrogen of MeQ$^+$ (Zn(1)−N(1) 2.153(3) Å), and the axial fluoride (Zn(1)−F(1) 2.447 Å).

Interestingly the observed Zn···F separations (av 2.332 Å) are considerably longer than that of a Zn−F covalent bond (~1.775 Å). Similarly the P···F distances observed in **3** (av 2.939 Å) are almost twice those of the covalent P−F bonds (~1.56 Å as in PF$_3$).[16] These values suggest that the zinc centers of the cubane are far more affected than the phosphorus

Table 1. Comparison of the Dimensions of Cores of Various D4R Cubanes and the Interaction of Fluoride Ion with Cage Atoms

| $F@Si_8$	$F@Ge_8$	$F@Zn_4P_4$	Zn_4P_4
$F@[RSiO_{1.5}]_8$ (R = vinyl)[9f]	$F@[Ge_8O_{12}(OH)_8]$[10]	$F@[Zn(dipp)(MeQ)(DMSO)_3]_4$ (3)	$[Zn(dipp)(collidine)]_4$[13]
average distances (Å) and angles (deg)	average distances (Å) and angles (deg)	average distances (Å) and angles (deg)	average distances (Å) and angles (deg)
Si···Si (edge), 3.058k	Ge···Ge (edge), 3.185	Zn···P (edge), 3.095	Zn···P (edge), 3.196
Si···Si (face diagonal), 4.325	Ge···Ge (face diagonal), 4.467	Zn···Zn (face diagonal), 3.850	Zn···Zn (face diagonal), 4.419
Si···Si (body diagonal), 5.301	Ge···Ge (body diagonal), 5.512	P···P (face diagonal), 4.780	P···P (face diagonal), 4.632
Si···F, 2.65	Ge···F, 2.760	Zn···P (body diagonal), 5.277	Zn···P (body diagonal), 5.529
∠ O−Si−O (cage), 112.6	∠ O−Ge−O (cage), 115.8	Zn···F, 2.332; P···F, 2.939	∠ O−Zn−O (cage), 111.6
∠ C−Si−O, 106.1	∠ O−Ge−O, 102.0	∠ O−Zn−O (cage), 119.3	

centers by the fluoride incorporation (all phosphorus atoms are left in the original tetrahedral geometry). The entry of fluoride ion into the cage thus brings about a distortion in the cubane structure by fluoride drawing zinc centers closer to it without disturbing the phosphorus centers. As a result the Zn···Zn face diagonal distance falls to 3.85 Å while the P···P face diagonal stays at 4.78 Å. In the parent cubane with no fluoride ion incorporation these values are 4.32 and 4.61 Å, respectively.[13]

Table 1 depicts a further comparison of the dimensions of the cubane core **3** vis-à-vis $F@Si_8$ and $F@Ge_8$ systems reported in the literature.[9,10] The major difference between **3** and the other two examples is the symmetric nature of the D4R cubane itself. While the cubane symmetry is more or less preserved in the Si and Ge cubanes even after the encapsulation of fluoride anion, the zinc phosphate cubane undergoes a structural change so as to enhance fluoride to zinc centers interaction. This is easily reflected in significantly shorter Zn···F distances in **3** (av 2.332 Å) compared to longer Si···F and Ge···F distances (av 2.65 and 2.76 Å, respectively). As a consequence, Si and Ge centers in $F@Si_8$ and $F@Ge_8$ retain their tetrahedral geometry, while the zinc centers in **3** adopt tbp geometry after fluoride incorporation. The unique ability of preformed **1** to encapsulate fluoride (unlike the incorporation of fluoride in the cage formation stages in the case of the Si_8 and Ge_8 systems) can be attributed to the Lewis acidity of tetrahedral zinc ions.

Synthesis and Spectra of Compounds 4−6 and the Test of Selectivity. The use of $[MeQ]SbF_6$ as the source of fluoride ion as well as N-donor ligand for the synthesis and structural characterization of **3** impelled the possibility of introducing a second positive charge on the cubane by using an extra equivalent of MeQ^+ in the reaction. Such an approach would also offer an opportunity to introduce a second anion, albeit present outside the cubane. This would in turn allow the evaluation of the selectivity of D4R cages for the F⁻ anion over the other anions. To verify this hypothesis (Scheme 2), compound **1** was treated with 2 equiv of $[MeQ]I$ followed by the addition of a fluoride source. The use of $^nBu_4NF$ as the fluoride ion source leads to the isolation of $[F@\{Zn_4(dipp)_4-(MeQ)_2(CH_3OH)_2\}][I]$ (**4**), whereas $NaBF_4$ as the F⁻ ion source yields $[F@\{Zn_4(dipp)_4(MeQ)_2(CH_3OH)_2\}][BF_4]$ (**5**). The change of viologen to $[MeQ][PF_6]$ in the presence of

Scheme 2. Synthesis of Neutral (Zwitterionic) 3 and Cationic 4−6

4, X^1 = I, Y = TBA-F, and X^2 = I
5, X^1 = I, Y = NaBF₄, and X^2 = BF₄
6, X^1 = PF₆, Y = TBA-F, and X^2 = PF₆
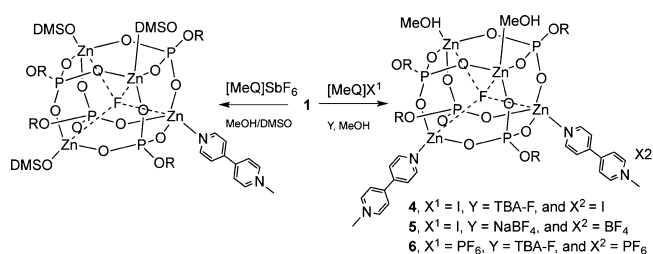
$^nBu_4NF$ results in $[F@\{Zn_4(dipp)_4(MeQ)_2(CH_3OH)_2\}][PF_6]$ (**6**). Compounds **4** and **5** have been obtained as single crystals, and their crystal structures have been determined (Figures 6 and 7). The formation of compounds **4−6** with fluoride ion
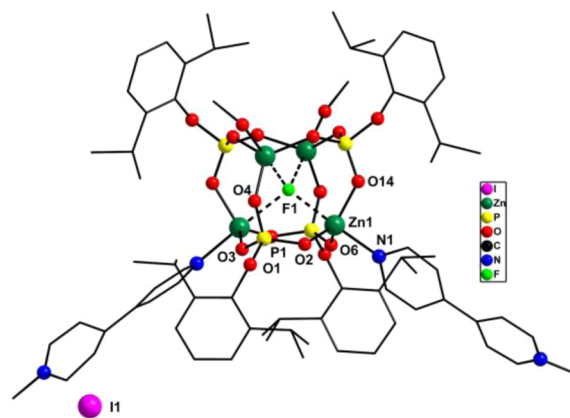
Figure 6. Molecular structure of compound **4**. Selected bond distances [Å]: Zn−O 1.905(7)−2.010(6) (av 1.961), P−O(Zn) 1.482(7)−1.588(7) (av 1.530), P−O(Ar) 1.616(7)−1.646(7) (av 1.631), Zn−F 2.276(5)−2.450(5) (av 2.356), P−F 2.960(6)−3.005(6) (av 2.989); bond angles [deg]: O−Zn−O (equatorial) 109.20(3)−130.40(3) (av119.67), O−Zn−O (axial) 92.90(3)−94.70(3) (av 94.03), N−Zn−O 90.40(3)−97.60(3) (av 93.56), F−Zn−O (equatorial) 84.10(2)−88.60(2) (av 86.83), N−Zn−F 173.30(2)−174.4(2) (av 173.85), ∠P 103.10(4)−114.0(4) (av109.23), ∠ Zn−O−P 119.50(4)−134.10(4) (av 127.05).
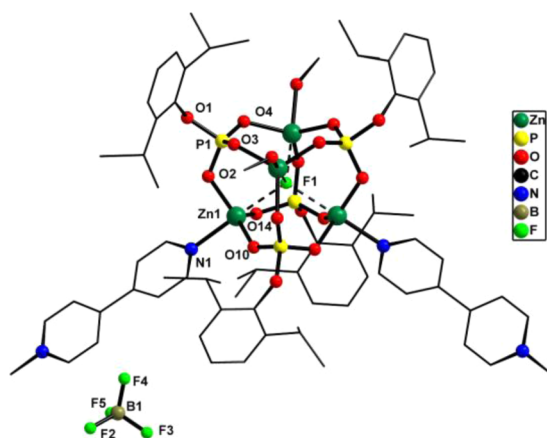
Figure 7. Molecular structure of **5**. Selected bond distances [Å]: Zn–O 1.943(6)–1.967(5) (av 1.953), P–O(Zn) 1.495(6)–1.526(6) (av 1.514), P–O(Ar) 1.599(5)–1.641(7) (av 1.619), Zn–F 2.245 (4)–2.407(4) (av 2.331), P–F 2.977(2)–3.021(2) (av 3.009); bond angles [deg]: O–Zn–O (equatorial) 109.50(2)–129.30(2) (av119.80), O–Zn–O (axial) 89.20(2)–93.30(2) (av 90.90), N–Zn–O 89.30(2)–96.50(3) (av 92.83), F–Zn–O (equatorial) 84.57(2)–89.53(2) (av 87.56), N–Zn–F 173.10(2)–175.7(2) (av 174.40), ∠P 103.50(3)–115.90 (4) (av109.18), Zn–O–P 119.80(3)–133.40(4) (av 126.14).

inside the cage and the second anion (iodide, tetrafluoroborate, and hexafluorophosphate, respectively) outside the cage clearly underscores the selectivity of the D4R cubane to encapsulate only fluoride and leave any other anions outside the cage.

The cationic fluoride-incorporated cubanes **4–6** were characterized by elemental analysis, FT-IR, and ^{1}H and ^{31}P NMR spectroscopic methods (Supporting Information, Table S1). Clusters **4–6** were probed by negative ion ESI mass spectrometry to confirm fluoride incorporation (Supporting Information, Figures S5–S7). The observed FT-IR spectra are similar to that of **2** (Figure 3).[14] The ^{1}H and ^{31}P NMR spectra of **4–6** show spectral behavior similar to **3** (Supporting Information, Figures S8–S10). For **6**, two ^{31}P NMR signals are observed at 2.5 and −144 ppm; the former corresponds to the cubane phosphorus center as a singlet, and the latter corresponds to that center as a septet for the PF_6 anion (Supporting Information, Figure S10). Similar to the spectra of compounds **2** and **3**, a single resonance at −113 ppm in the ^{19}F NMR spectrum of **4** indicates the presence of only one type of fluoride (Supporting Information, Figure S8). In the ^{19}F NMR spectrum of **5**, while the signal at −113 ppm is due to D4R-encapsulated fluoride, two signals with the intensity ratio of 1:5 at −148 and −148.2 ppm are assignable to the [10]B- and [11]B-coupled fluorine of the BF_4^- anion (Supporting Information, Figure S9).[17] In the ^{19}F NMR spectrum of **6**, apart from the expected F@D4R resonance at −113 ppm, the doublet observed at −70 ppm (J = 711 Hz) is assignable to the phosphorus-coupled signal of the PF_6^- anion (Supporting Information, Figure S10).[18,19]

Molecular Structures of Compounds 4 and 5. Compounds **4** and **5** crystallize in monoclinic $P2_1/c$ space group. There are two different types of Zn centers present in the asymmetric unit of **4** and **5** (Figures 6 and 7; Supporting Information, Figures S11 and S12). Similar to compound **3**, all Zn centers in **4** and **5** adopt tbp geometry, with one of the axial positions occupied by fluoride. The bond distances and angles observed for **4** and **5** are similar to those described above for **3**. The most significant outcome of structural studies on **4** and **5** is

the proof (in the solid state) of the ability of the cubane to encapsulate only fluoride ion and keep other anions such as I$^-$ and BF_4^- outside the cage.

Thermal Analyses. Thermogravimetric analysis (TGA) of compound **2** under N_2 atmosphere reveals a weight loss of ~67.5% in the range of 100−500 °C, corresponding to the loss of all organic substituents and water molecules, leading to the formation of zinc pyrophosphate $[Zn_2P_2O7]_{0.5}$ (~32%, calculated from molecular formula).[20] Compounds **3–6** show similar thermal behavior, and the remaining ceramic material obtained in each case corresponds to the zinc pyrophosphate. Figure 8 shows TGA plots of **2–6** at a heating rate of 10 °C/min under N_2 atmosphere.
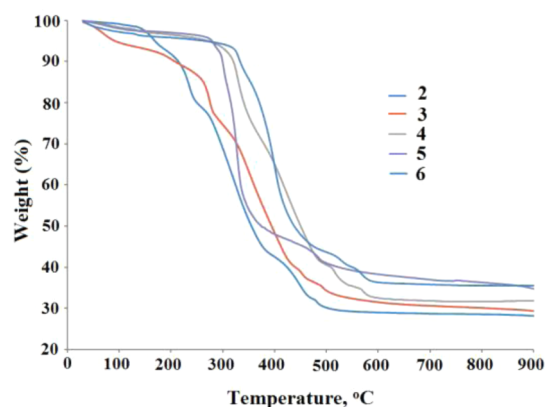
Figure 8. TGA plots of **2–6** at heating rate of 10 °C/min under N_2.

Possible Applications: Sensing Fluoride Present in Water and Toothpaste. The ability of compounds **2–6** not only in encapsulating fluoride ions but also in excluding other larger anions points to possible applications for the D4R zinc phosphate cubanes. Since anything in excess of 4 mg/L or 4 ppm of NaF in drinking water can lead to adverse health effects, cubane **1** was tested for its ability to pick up fluoride ions from aqueous medium through ^{19}F NMR titration of NaF dissolved in water against **1** (Figure 9). The fluoride ion in water gives a single resonance at −144.0 ppm, which on addition of **1** shifts to −113.5 ppm due to the incorporation of fluoride ions inside
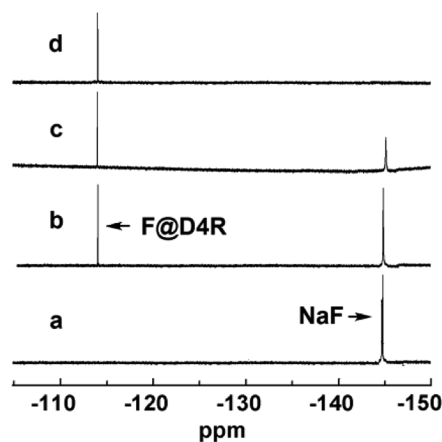
Figure 9. The ^{19}F NMR spectrum (CD$_3$OD) of 3.3 × 10$^{−5}$ M solution of NaF dissolved in water with the following concentrations of compound **1**: (a) none; (b) 1.3 × 10$^{−5}$ M; (c) 2.6 × 10$^{−4}$ M; (d) 4 × 10$^{−5}$ M.

the cage. When all fluoride ions have been incorporated inside the cage, the resonance at −144.0 ppm completely disappears, thus giving the exact F⁻ ion concentration in water.

A similar experiment was also performed to determine the amount of fluoride ion present in commercial toothpastes. Cubane **1** was treated with DMSO extracts of an anticavity toothpaste containing Na_2PFO_3. The ^{31}P NMR spectrum in this case (Figure 10) clearly shows a new peak at 2.5 ppm,
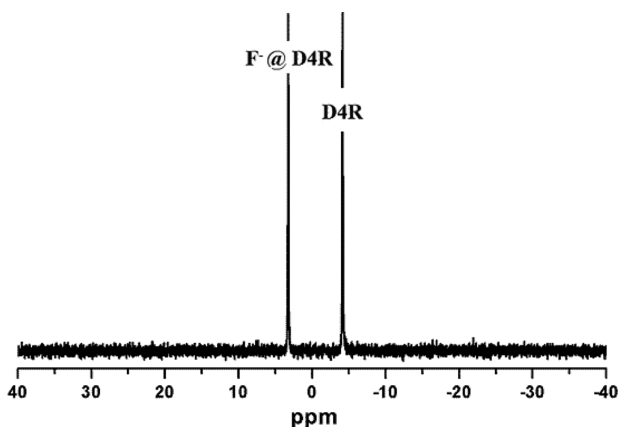
Figure 10. ^{31}P NMR spectrum (DMSO-d_6) of $[Zn(dipp)(DMSO)]_4$ after adding toothpaste extract containing Na_2PFO_3.

confirming fluoride encapsulation. This once again demonstrates the fluoride ion scavenging capabilities of **1** from a variety of fluoride sources.

Conclusions. In summary, we demonstrated that the preformed D4R zinc phosphate molecular clusters play host to fluoride ions in solution and in solid state, with the resultant F@D4R structures being stabilized in anionic (as in **2**), neutral (as in **3**), and cationic (as in **4−6**) forms. It was further shown that fluoride ion source can vary from organic soluble $^nBu_4NF$ (or even $[MeQ]SbF_6$) to inorganic fluorides such as NaF (the source of fluoride ions in drinking water) and Na_2PFO_3 (commonly found in toothpastes). This is the first report on the usage of preformed D4R structure for the purposes of anion sensing and scavenging in a neat fashion under ambient conditions. A simple technique such as NMR spectroscopy (exceptional detection limits) can be used to quantitatively determine the incorporation both in aqueous and organic media by using either phosphorus or fluorine probes, complementing other types of fluoride sensors reported in the literature that use other techniques for sensing action.[21]

■ EXPERIMENTAL SECTION

Instruments and Methods. All reactions were carried out under fume hood in beakers or round-bottom flasks without any special precautions, if not stated otherwise. All the starting materials and the products were found to be stable toward moisture and air, and no specific precaution was taken to rigorously exclude air. The melting points were measured in glass capillaries. Infrared spectra were obtained on a Perkin-Elmer Spectrum One FT-IR spectrometer as KBr diluted discs. Microanalyses were performed on a Thermo Finnigan (FLASH EA 1112) microanalyzer. NMR spectra were recorded using a Bruker Advance DPX-400 spectrometer, and the peaks that are not labeled are always solvent peaks, if not stated otherwise. Thermo gravimetric analyses were carried out with a Perkin-Elmer thermal analysis system, under a stream of nitrogen gas, at the heating rate of 10 °C/min. Commercial-grade solvents were purified by employing standard procedures. Other chemicals such as 2,6-di-*iso*-propylphenol

(Sigma Aldrich), $Zn(OAc)_2·2H_2O$ (S.d.Fine-Chem.), 4,4′-bipyridine (Sigma Aldrich), methyl iodide (Sigma Aldrich), tetrabutyl ammonium fluoride ($^nBu_4NF$) (Sigma Aldrich), $NaBF_4$ (Alfa Aesar), $AgSbF_6$ (Sigma Aldrich), and NH_4PF_6 (Sigma Aldrich) were used as received. The 2,6-di-*iso*-propylphenyl phosphate and the bipyridinium methyl salts, for example, 1-methyl-4,4′-bipyridin-1-ium iodide (MeQI), 1-methyl-4,4′-bipyridin-1-ium hexafluorophosphate (MeQPF₆), and 1-methyl-4,4′-bipyridin-1-ium hexafluoroantimonate (MeQSbF₆), were synthesized according to the reported methods.[22,23]

[$^nBu_4N$][F@{Zn(dipp)(DMSO)}₄] (2). $[Zn(dipp)(DMSO)]_4$ (**1**) (0.025 g, 0.016 mmol) was dissolved in methanol (20 mL), and a saturated solution of $^nBu_4NF$ in methanol (5 mL) was added, stirred, and kept for crystallization on benchtop to obtain colorless crystals of compound **2** after 2 d. mp: >250 °C. Yield: 0.025 g (83%). Anal. Calcd for $C_{72}H_{128}FNO_{20}P_4S_4Zn_4$ (M_r = 1860.52) (%): C, 46.48; H, 6.93; S, 6.89. Found: C, 47.06; H, 6.47; S, 6.71. FT-IR (KBr, cm⁻¹): 2961 (vs), 2868 (s), 1652 (br), 1447 (s), 1383 (s), 1256 (s), 1156 (vs), 1037 (vs), 995 (vs), 908 (vs), 769 (vs), and 564 (vs). ^1H NMR (DMSO-d_6, 400 MHz): δ 6.9 (m, 12H, Ar), 3.8 (septet, 8H, $^3J_{HH}$ = 6.8 Hz, ^iPr−CH), 3.1 (t, 8H, $^3J_{HH}$ = 6.9 Hz, −CH₂), 1.5 (m, 8H, $^3J_{HH}$ = 7.6 Hz, −CH₂), 1.3 (m, 8H, $^3J_{HH}$ = 7.3 Hz, −CH₂), 1.05 (d, 48H, ^3J = 6.9 Hz, ^iPr−CH₃), 0.9 (t, 12H, $^3J_{HH}$ = 7.2 Hz, −CH₃) ppm. ^{31}P NMR (DMSO-d_6, 161 MHz): δ 3.2 ppm. ^{19}F NMR (DMSO-d_6, 400 MHz): δ −113 (s, 1F, F@D4R) ppm. ESI MS (-ve): calculated for [M-4DMSO]⁻, m/z 1305, found 1305.

[F@{Zn₄(dipp)₄(MeQ)(DMSO)₃}] (3). Compound **1** (0.04 g, 0.025 mmol) was dissolved in methanol (20 mL), and a solution of [MeQ][SbF₆] (0.04 g, 0.1 mmol) in methanol (15 mL) was added, stirred, and kept on benchtop to yield colorless crystals of compound **2** after 4−5 d. mp: >250 °C. Yield: 0.035 g (83%). Anal. Calcd for $C_{65}H_{97}FN_2O_{19}P_4S_3Zn_4$ (M_r = 1711.14) (%): C, 45.62; H, 5.71; N, 1.64. Found: C, 45.68; H, 6.16; N, 1.48. FT-IR (KBr, cm⁻¹): 3434 (br), 2962 (vs), 2867 (s), 1647 (s), 1613 (s), 1467 (s), 1441 (s), 1337 (s), 1256 (s), 1156 (vs), 996 (vs), 911 (vs), 822 (s), 769 (vs), 743 (vs), and 564 (s). ^1H NMR (DMSO-d_6, 400 MHz): δ 9.0 (d, 2H, ^3J = 6.6 Hz, *ortho*-N⁺), 8.8 (d, 2H, ^3J = 6.1 Hz, *ortho*-N), 8.5 (d, 2H, ^3J = 6.6 Hz, *meta*-N⁺), 7.9 (d, 2H, ^3J = 6.1 Hz, *meta*-N⁺), 6.9 (m, 12H, Ar), 4.2 (s, 3H, CH₃−N⁺), 3.3 (septet, 8H, $^3J_{HH}$ = 6.7 Hz, ^iPr−CH), and 1.06 (d, 48H, $^3J_{HH}$ = 6.9 Hz, ^iPr−CH₃) ppm. ^{31}P NMR (DMSO-d_6, 161 MHz): δ 3.0 ppm. ^{19}F NMR (DMSO-d_6, 400 MHz): δ −113 (s, 1F, F@D4R) ppm. ESI MS (-ve): calculated for [M-MeQ-3DMSO]⁻, m/z 1305, found 1305.

[F@{Zn₄(dipp)₄(MeQ)₂(CH₃OH)₂}][I]·3CH₃OH (4). To a solution of compound **1** (0.025 g, 0.016 mmol) in methanol (20 mL), [MeQ]I (0.0360 g, 0.12 mmol) was added. The solution was further diluted with methanol (80 mL), and a saturated solution of $^nBu_4NF$ in methanol (5 mL) was added slowly. The resulting solution was kept for crystallization. After 5 d, compound **4** was obtained as yellowish crystal. mp: >250 °C. Yield: 0.026 g (86%). Anal. Calcd for $C_{75}H_{110}FIN_4O_{21}P_4Zn_4$ (M_r = 1935.07) (%): C, 46.55; H, 5.73; N, 2.90. Found: C, 46.07; H, 5.20; N, 2.71. FT-IR (KBr, cm⁻¹): 2963 (vs), 2867 (s), 1644 (s), 1615 (s), 1441 (s), 1335 (s), 1256 (s), 1156 (vs), 997 (vs), 912 (vs), 772 (s), and 565 (s). ^1H NMR (DMSO-d_6, 400 MHz): δ 9.1 (d, 4H, $^3J_{HH}$ = 6.8 Hz, *ortho*-N⁺), 8.8 (d, 4H, $^3J_{HH}$ = 6.2 Hz, *ortho*-N), 8.5 (d, 4H, $^3J_{HH}$ = 6.9 Hz, *meta*-N⁺), 8.0 (d, 4H, $^3J_{HH}$ = 6.2 Hz, *meta*-N⁺), 7.0 (m, 12H, Ar), 4.3 (s, 6H, CH₃−N⁺), 3.8 (septet, 8H, $^3J_{HH}$ = 6.8 Hz, ^iPr−CH), 1.05 (d, 48H, $^3J_{HH}$ = 6.8 Hz, ^iPr−CH₃) ppm. ^{31}P NMR (DMSO-d_6, 161 MHz): δ 2.5 ppm. ^{19}F NMR (DMSO-d_6, 400 MHz): δ −113 (s, 1F, F@D4R) ppm. ESI MS (-ve): calculated for [M-2MeQ-5CH₃OH-I]⁻, m/z 1305, found 1305.

[F@{Zn₄(dipp)₄(MeQ)₂(CH₃OH)₂}][BF₄] (5). To a solution of compound **1** (0.04 g, 0.025 mmol) in methanol (20 mL), [MeQ]I (0.04 g, 0.12 mmol) was added, and the solution was further diluted with methanol (150 mL). A saturated solution of $NaBF_4$ in methanol (5 mL) was added, and the resulting solution was kept for crystallization. The product was obtained as platelike crystals after 15 d. mp: >250 °C. Yield: 0.038 g (84%). Anal. Calcd for $C_{72}H_{98}BF_5N_4O_{18}P_4Zn_4$ (M_r = 1798.84) (%): C, 48.07; H, 5.49; N, 3.11. Found: C, 48.04; H, 4.93; N, 3.01. FT-IR (KBr, cm⁻¹): 2963 (vs), 2866 (s), 1647 (s), 1614 (s), 1439 (s), 1417(s), 1335 (s), 1256

Table 2. Crystal Data and Structure Refinement Details for Compounds 3−5

compound	3	4[a]	5
identification code	rm359	ak642	ak186mp
formula	$C_{65}H_{97}F N_2O_{19}P_4S_3Zn_4$	$C_{72}H_{98}F_1I_1N_4O_{18}P_4Zn_4$	$C_{72}H_{98}BF_5N_4O_{18}P_4Zn_4$
Fw	1710.99	1838.80	1798.71
temp, [K]	150(2)	150(2)	150(2)
crystal system	orthorhombic	monoclinic	monoclinic
space group	$P2_12_12_1$	$P 2_1/c$	$P 2_1/c$
a, [Å]	15.030(4)	21.480(2)	21.118(2)
b, [Å]	21.704(7)	15.268(2)	15.064(1)
c, [Å]	24.470(6)	31.930(4)	31.417(4)
α, [deg]	90	90	90
β, [deg]	90	97.689(1)	97.306(1)
γ, [deg]	90	90	90
V, [Å³]	7982(4)	10378(2)	9913(2)
Z	4	4	4
D (calcd), [g/cm³]	1.424	1.177	1.205
μ [mm⁻¹]	1.413	1.326	1.085
crystal size, [mm³]	0.36 × 0.33 × 0.28	0.16 × 0.15 × 0.08	0.37 × 0.04 × 0.03
θ range, [deg]	3.32 to 25.00	1.81 to 25.00	2.87 to 25.00
no. of rflns collected	58 068	55 298	58 910
independent reflns $(I_0 > 2\sigma(I_0))$	14 011	17 925	16 193
GOF	0.819	1.084	0.683
$R1(I_0 > 2\sigma(I_0))$	0.0425	0.1318	0.0631
$wR2$ (all data)	0.0812	0.3713	0.1463
largest hole and peak [e·Å⁻³]	−0.406 and 0.553	−0.975 and 1.857	−0.398 and 0.943

[a]Poor quality data; see Experimental Section for details.

(s), 1147 (vs), 991 (vs), 905 (vs), 771 (vs), and 609 (s). ^{1}H NMR (DMSO-d_6, 400 MHz): δ 9.1 (d, 4H, $^3J_{HH}$ = 6.4 Hz, *ortho*-N⁺), 8.8 (d, 4H, $^3J_{HH}$ = 6.1 Hz, *ortho*-N), 8.6 (d, 4H, $^3J_{HH}$ = 6.9 Hz, *meta*-N⁺), 8.0 (d, 4H, $^3J_{HH}$ = 6.1 Hz, *meta*-N⁺), 7.0 (m, 12H, Ar), 4.38 (s, 6H, CH₃−N⁺), 3.6 (septet, 8H, $^3J_{HH}$ = 7.1 Hz, ^{i}Pr−CH), 1.1 (d, 48H, $^3J_{HH}$ = 6.9 Hz, ^{i}Pr−CH₃) ppm. ^{31}P NMR (DMSO-d_6, 161 MHz): δ 2.5 ppm. ^{19}F NMR (DMSO-d_6, 400 MHz): δ −113 (s, 1F, F@D4R) and −148.1 (two peaks with intensity ratio of 0.22:1 because of the coupling with ^{10}B and ^{11}B, 4F, BF₄) ppm. ^{11}B NMR (DMSO-d_6, 128 MHz): δ −1.25 ppm. ESI MS (-ve): calculated for [M-2MeQ-2CH₃OH-BF₄]⁻, m/z 1305, found 1305.

[F@{Zn₄(dipp)₄(MeQ)₂(CH₃OH)₂}] [PF₆] (6). To a solution of compound **1** (0.04 g, 0.025 mmol) in methanol (20 mL), [MeQ]PF₆ (0.03 g, 0.1 mmol) was added and diluted with methanol (80 mL). A saturated solution of ^{n}Bu₄NF in methanol (5 mL) was added, and the resulting solution was kept for crystallization. After 2 d the product was obtained as white crystals. mp: >250 °C. Yield: 0.040 g (87%). Anal. Calcd for C₇₂H₉₈F₇N₄O₁₈P₅Zn₄ (M_r = 1857.00) (%): C, 46.57; H, 5.32; N, 3.02. Found: C, 46.13; H, 4.91; N, 3.13. FT-IR (KBr, cm⁻¹): 2963 (vs), 2868 (s), 1708 (s), 1615 (s), 1466 (s), 1336 (s), 1223 (s), 1154 (vs), 997 (vs), 909 (vs), 843 (vs), 774 (s), and 558 (vs). ^{1}H NMR (DMSO-d_6, 250 MHz): δ 9.1 (d, 4H, $^3J_{HH}$ = 6.7 Hz, *ortho*-N⁺), 8.8 (d, 4H, $^3J_{HH}$ = 6.1 Hz, *ortho*-N), 8.5 (d, 4H, $^3J_{HH}$ = 6.9 Hz, *meta*-N⁺), 7.9 (d, 4H, $^3J_{HH}$ = 6.2 Hz, *meta*-N⁺), 6.8 (m, 12H, Ar), 4.2 (s, 6H, CH₃−N⁺), 3.8 (septet, 8H, $^3J_{HH}$ = 6.8 Hz, ^{i}Pr−CH), 1.0 (d, 48H, ^3J = 6.8 Hz, ^{i}Pr−CH₃) ppm. ^{31}P NMR (DMSO-d_6, 100 MHz): δ 2.5 (s, 4P, dipp) and −144 (septet, 1P, $^1J_{PF}$ = 711 Hz, PF₆) ppm. ^{19}F NMR (DMSO-d_6, 400 MHz): δ −70 (d, 6F, $^1J_{PF}$ = 711 Hz, PF₆) and −113 (s, 1F, F@D4R) ppm. ESI MS (-ve): calculated for [M-2MeQ-2CH₃OH-PF₆]⁻, m/z 1305, found 1305.

Single-Crystal X-ray Diffraction Studies. A suitable colorless crystal of compound **3** (size: 0.36 × 0.33 × 0.28 mm³) obtained directly from the reaction mixture was mounted on an Oxford Xcalibur diffractometer equipped with Sapphire-III CCD camera for unit cell determination and three-dimensional intensity data collection. Data integration and indexing of **3** was done by using CrysAlisPro.[24] All calculations were carried out using the programs in the WinGX module[25] and solved by direct methods (SIR-92).[26] The final

refinement of the structure was carried out using full matrix least-squares methods on F^2 using SHELXL-97,[27] which resulted in the structure determination of **3**. The compound crystallizes in the orthorhombic $P2_12_12_1$ space group. The dipp moiety and the DMSO solvent show disorder, which has been resolved by dividing the atoms into two parts. The final refinement converged at the R value of 0.0442 ($I > 2\sigma(I)$).

Crystallization of the crude product of compound **4** from methanol at room temperature yields crystals of **4** as yellow block-type crystals. A suitable crystal of size 0.16 × 0.15 × 0.08 mm³ was mounted on a Rigaku Saturn 724+ ccd diffractometer for unit cell determination and three-dimensional intensity data collection. 800 frames in total were collected at 150 K with the exposure time of 24 s per frame. For the analysis, the detector was kept at a distance of 45 mm from the crystal. All calculations were carried out using the programs in WinGX module[25] and solved by direct methods (SIR-92).[26] The final refinement of the structure was carried out using full matrix least-squares methods on F^2 using SHELXL-97.[27] Unit cell determination using both high angle and low angle diffraction reveal that the compound crystallizes with the monoclinic $P2_1/c$ space group. The final refinement of the solved structure converged at the R value of 0.1318 ($I > 2\sigma(I)$). In the coordinated methanol molecule, the O−H protons are not added since refinement does not converge to zero after fixing the protons. Repeated crystallization and data collection could not give better R values due to highly fragile crystal quality (Table 2).

Data collection and structure solution and refinement for compound **5** using a suitable crystal of size 0.37 × 0.04 × 0.03 mm³, carried out in the same way as for compound **3**, reveals that this molecule crystallizes in monoclinic $P2_1/c$ space group. There were tetrahedral residual peaks in the molecule, but attempts to assign those residual peaks to the BF₄ anion were not successful. Since other characterization data was in agreement with the BF₄ anion, the molecule was squeezed and refined. The final refinement of the structure converged at the R value of 0.0631 ($I > 2\sigma(I)$). Final refinement data for compounds **3−5** are given in Table 2.

NMR Experiments. In the first experiment, 10^{-5} mol of [Zn(dipp)(DMSO)]₄ (**1**) was dissolved in 0.3 mL of CD₃OD in an

NMR tube, and the ^{31}P NMR spectrum was recorded. This solution was titrated against a known concentration of [NBu$_4$]F in CD$_3$OD using a micro pipet (Figure 1). In the second experiment, a 1×10^{-5} M solution of [Zn(dipp)(DMSO)]$_4$ (**1**) was dissolved in 0.4 mL of DMSO-d_6 in an NMR tube, and the ^{19}F NMR spectrum was recorded. This solution was titrated against a known concentration of [Zn(dipp)(DMSO)]$_4$ (**1**) (Figure 2). In the third experiment, [Zn(dipp)(DMSO)]$_4$ (**1**) was dissolved in CD$_3$OD, and to it a water solution of NaF was added. The solution was subjected to NMR spectroscopic analysis (Figure 8). In the fourth experiment [Zn-(dipp)(DMSO)]$_4$ (**1**) was treated with DMSO extracts of an anticavity toothpaste (Colgate toothpaste) containing Na$_2$PFO$_3$. ^{31}P NMR shows encapsulated cubane (Figure 9).

ASSOCIATED CONTENT

Ⓢ Supporting Information

This includes: FT-IR, ^{1}H and ^{31}P NMR spectra, ESI-MS spectra of **2**−**6**, and TGA plots of **2**−**6**. Crystallographic data of **3**−**5**. CCDC 959362−959364. This material is available free of charge via the Internet at http://pubs.acs.org.

AUTHOR INFORMATION

Corresponding Author

*E-mail: rmv@chem.iitb.ac.in. Phone: +91 22 2576 7163. Fax: +91 22 25767152.

Notes

The authors declare no competing financial interest.

ACKNOWLEDGMENTS

ABBREVIATIONS

DippH$_2$, 2,6-di-*iso*-propylphenyldihydrogenphosphate; s, sharp; vs, very sharp; w, weak; MeQ, 1-methyl-4,4′-bipyridin-1-ium cation

REFERENCES

(1) (a) Park, C. H.; Simmons, H. E. *J. Am. Chem. Soc.* **1968**, *90*, 2431. (b) Fainberg, A. *Science* **1992**, *255*, 1531. (c) Yinon, J. *Anal. Chem.* **2003**, *75*, 98A. (d) Singh, S. *J. Hazard. Mater.* **2007**, *144*, 15. (e) Senesac, L.; Thundat, T. G. *Mater. Today* **2008**, *11*, 28. (f) Qu, W. G.; Deng, B.; Zhong, S. L.; Shi, H.; Wang, S. S.; Xu, A. W. *Chem. Commun.* **2011**, *47*, 1237.

(2) (a) Salinas, Y.; Martínez-Máñez, R.; Marcos, M. D.; Sancenón, F.; Costero, A. M.; Parra, M.; Gil, S. *Chem. Soc. Rev.* **2012**, *41*, 1261. (b) Venkatramaiah, N.; Kumar, S.; Patil, S. *Chem. Commun.* **2012**, *48*, 5007. (c) Germain, M. E.; Knapp, M. J. *Chem. Soc. Rev.* **2009**, *38*, 2543.

(3) (a) Lavigne, J. J.; Anslyn, E. V. *Angew. Chem., Int. Ed.* **2001**, *40*, 3118. (b) Beer, P. D.; Gale, P. A. *Angew. Chem., Int. Ed.* **2001**, *40*, 486. (c) Gale, P. A.; Sessler, J. L. *Chem. Commun.* **1998**, 1. (d) De Silva, A. P.; Gunaratne, H. Q. N.; Gunnlaugsson, T.; Huxley, A. J. M.; McCoy, C. P.; Rademacher, J. T.; Rice, T. E. *Chem. Rev.* **1997**, *97*, 1515. (e) Schmidtchen, F. P.; Gleich, A.; Schummer, A. *Pure Appl. Chem.* **1989**, *61*, 1535.

(4) (a) United Nations Environment Programme. *Environmental Health Criteria 227: Fluoride;* ; International Labour Organization; WHO: Geneva, Switzerland, 2002; p 100. ISBN 9241572272. (b) Reddy, D. R. *Neurol. India* **2009**, *57*, 7.

(5) (a) National Research Council. *Fluoride in Drinking Water: A Scientific Review of EPA's Standards;* The National Academies Press: Washington, DC, 2006. (b) Gessner, B. D.; Beller, M.; Middaugh, J. P.; Whitford, G. M. *N. Engl. J. Med.* **1994**, *330*, 95.

(6) (a) Cametti, M.; Rissanen, K. *Chem. Soc. Rev.* **2013**, *42*, 2016. (b) Busschaert, N.; Wenzel, M.; Light, M. E.; Iglesias-Hernandez, P.; Perez-Tomas, R.; Gale, P. A. *J. Am. Chem. Soc.* **2011**, *133*, 14136. (c) Ravikumar, I.; Lakshminarayanan, P. S.; Arunachalam, M.; Suresh, E.; Ghosh, P. *Dalton Trans.* **2009**, 4160. (d) Kuk Kim, S.; Sessler, J. L.; Gross, D. E.; Lee, C.-H.; Kim, J. S.; Lynch, V. M.; Delmau, L. H.; Hay, B. P. *J. Am. Chem. Soc.* **2010**, *132*, 5827. (e) Arunachalam, M.; Ghosh, P. *Inorg. Chem.* **2010**, *49*, 943. (f) Kang, S. O.; Day, V. W.; Bowman-James, K. *Org. Lett.* **2008**, *10*, 2677.

(7) Päch, M.; Stosser, R. *J. Phys. Chem. A* **1997**, *101*, 8360.

(8) Bassindale, A. R.; Pourny, M.; Taylor, P. G.; Hursthouse, M. B.; Light, M. E. *Angew. Chem., Int. Ed.* **2003**, *42*, 3487.

(9) (a) Anderson, S. E.; Bodzin, D. J.; Haddad, T. S.; Boatz, J. A.; Mabry, J. M.; Mitchell, C.; Bowers, M. T. *Chem. Mater.* **2008**, *20*, 4299. (b) Aziz, Y. E.; Bassindale, A. R.; Taylor, P. G.; Horton, P. N.; Stephenson, R. A.; Hursthouse, M. B. *Organometallics* **2012**, *31*, 6032. (c) Bassindale, A. R.; Liu, Z.; MacKinnon, I. A.; Taylor, P. G.; Yang, Y.; Light, M. E.; Horton, P. N.; Hursthouse, M. B. *Dalton Trans.* **2003**, 2945. (d) Bassindale, A. R.; Chen, H.; Liu, Z.; MacKinnon, I. A.; Parker, D. J.; Taylor, P. G.; Yang, Y.; Light, M. E.; Horton, P. N.; Hursthouse, M. B. *J. Organomet. Chem.* **2004**, *689*, 3287. (e) Bassindale, A. R.; Parker, D. J.; Pourny, M.; Taylor, P. G.; Horton, P. N.; Hursthouse, M. B. *Organometallics* **2004**, *23*, 4400. (f) Bassindale, A. R.; Pourny, M.; Taylor, P. G.; Hursthouse, M. B.; Light, M. E. *Angew. Chem., Int. Ed.* **2003**, *42*, 3488. (g) Mabry, J. M.; Iacono, S. T.; Viers, B. D. *Angew. Chem., Int. Ed.* **2008**, *4*, 4137. (h) Bauzá, A.; Mooibroek, T. J.; Frontera, A. *Angew. Chem., Int. Ed.* **2013**, *52*, 12317.

(10) Villaescusa, L. A.; Lightfoot, P.; Morris, R. E. *Chem. Commun.* **2002**, 2220.

(11) Riou, D.; Taulelle, F.; Ferey, G. *Inorg. Chem.* **1996**, *35*, 6392.

(12) (a) Reinert, P.; Patarin, J.; Loiseau, T.; Ferey, G.; Kessler, H. *Microporous Mesoporous Mater.* **1998**, *22*, 43. (b) Loiseau, T.; Ferey, G. *J. Mater. Chem.* **1996**, *6*, 1073. (c) Loiseau, T.; Ferey, G. *J. Solid State Chem.* **1994**, *111*, 403. (d) Walton, R. I.; Millange, F.; Bail, A. L.; Loiseau, T.; Serre, C.; O'Hare, D.; Ferey, G. *Chem. Commun.* **2000**, 203. (e) Taulelle, F.; Poblet, J.-M.; Ferey, G.; Benard, M. *J. Am. Chem. Soc.* **2001**, *123*, 111. (f) Matijasic, A.; Paillaud, J.-L.; Patarin, J. *J. Mater. Chem.* **2000**, *10*, 1345. (g) Reinert, P.; Patarin, J. *J. Mater. Sci.* **2000**, *35*, 2965.

(13) Chang, W. K.; Wur, C. S.; Wang, S. L.; Chiang, R. K. *Inorg. Chem.* **2006**, *45*, 6622.

(14) (a) Murugavel, R.; Kuppuswamy, S.; Boomishankar, R.; Steiner, A. *Angew. Chem., Int. Ed.* **2006**, *45*, 5536. (b) Murugavel, R.; Kuppuswamy, S.; Gogoi, N.; Boomishankar, R.; Steiner, A. *Chem.— Eur. J.* **2010**, *16*, 994. (c) Murugavel, R.; Kuppuswamy, S.; Gogoi, N.; Steiner, A. *Inorg. Chem.* **2010**, *49*, 2153. (d) Murugavel, R.; Walawalkar, M. G.; Pothiraja, R.; Rao, C. N. R.; Choudhury, A. *Chem. Rev.* **2008**, *108*, 3549. (e) Murugavel, R.; Kuppuswamy, S. *Angew. Chem., Int. Ed.* **2006**, *45*, 7022. (f) Murugavel, R.; Kuppuswamy, S.; Gogoi, N.; Boomishankar, R.; Steiner, A. *Chem.— Eur. J.* **2008**, *14*, 3869. (g) Kalita, A. C.; Roch-Marchal, C.; Murugavel, R. *Dalton. Trans* **2013**, *42*, 9755. (h) Murugavel, R.; Kuppuswamy, S. *Inorg. Chem.* **2008**, *47*, 7686. (i) Murugavel, R.; Kuppuswamy, S.; Randoll, S. *Inorg. Chem.* **2008**, *47*, 6028. (j) Murugavel, R.; Kuppuswamy, S.; Maity, A. N.; Sing, M. P. *Inorg. Chem.* **2009**, *48*, 183.

(15) (a) Murugavel, R.; Shanmugan, S. *Chem. Commun.* **2007**, 1257. (b) Murugavel, R.; Shanmugan, S. *Dalton Trans.* **2008**, 5358. (c) Walawalkar, M. G.; Horchler, S.; Dietrich, S.; Chakraborty, D.; Roesky, H. W.; Schaefer, M.; Schmidt, H. G.; Sheldrick, G. M.; Murugavel, R. *Organometallics* **1998**, *17*, 2865. (d) Murugavel, R.; Walawalkar, M. G.; Dan, M.; Roesky, H. W.; Rao, C. N. R. *Acc. Chem. Res.* **2004**, *37*, 763. (e) Murugavel, R.; Gogoi, N.; Clerac, R. *Inorg. Chem.* **2009**, *48*, 646.

(16) Flory, M. A.; McLamarrah, S. K.; Ziurys, L. M. *J. Chem. Phys.* **2006**, *125*, 194304.

(17) (a) Falcone, R. D.; Baruah, B.; Gaidamauskas, E.; Rithner, C. D.; Correa, N. M.; Silber, J. J.; Crans, D. C.; Levinger, N. E. *Chem.—Eur. J.* **2011**, *17*, 6837. (b) Dolbier, W. R. *Guide to Fluorine NMR for Organic Synthesis;* John Wiley & Sons: Hoboken, NJ, 2009.

(18) For comparison, δ_F for $[N^nBu_4][SbF_6]$ in $CHCl_3$ is -119.9 ppm; see: Kim, J. H.; Lee, J. W.; Shin, U. S.; Lee, J. Y.; Leeb, S.; Song, C. E. *Chem. Commun.* **2007**, 4683.

(19) The δ_F for F@D4R alumino- or gallophosphate cages of molecular sieves is downfield at -69 to -95 ppm, although the ^{19}F chemical shift of the fluoride ion encapsulated in the germanium oxide D4R cage occurs at -15 ppm; see: (a) Reinert, P.; Marler, B.; Patarin, J. *Chem. Commun.* **1998**, 1769. (b) Schreyeck, L.; D'agosto, F.; Stumbe, J.; Caulet, P.; Mougenel, J. C. *Chem. Commun.* **1997**, 1241. (c) Matijasic, A.; Paillaud, J.-L.; Patarin, J. *J. Mater. Chem.* **2000**, *10*, 1345.

(20) (a) Pothiraja, R.; Sathiyendiran, M.; Butcher, R. J.; Murugavel, R. *Inorg. Chem.* **2005**, *44*, 6314. (b) Pothiraja, R.; Sathiyendiran, M.; Butcher, R. J.; Murugavel, R. *Inorg. Chem.* **2004**, *43*, 7585. (c) Murugavel, R.; Sathiyendiran, M.; Pothiraja, R.; Walawalkar, M. G.; Mallah, T.; Riviere, E. *Inorg. Chem.* **2004**, *43*, 945. (d) Sathiyendiran, M.; Murugavel, R. *Inorg. Chem.* **2002**, *41*, 6404. (e) Murugavel, R.; Sathiyendiran, M.; Walawalkar, M. G. *Inorg. Chem.* **2001**, *40*, 427.

(21) (a) Lee, D. H.; Lee, H. Y.; Lee, K. H.; Hong, J.-I. *Chem. Commun.* **2001**, 1188. (b) Sui, B.; Kim, B.; Zhang, Y.; Frazer, A.; Belfield, K. D. *ACS Appl. Mater. Interfaces* **2013**, *5*, 2920. (c) Ke, I.-S.; Myahkostupov, M.; Castellano, F. N.; Gabbaï, F. P. *J. Am. Chem. Soc.* **2012**, *134*, 15309. (d) Yong, X.; Su, M.; Wang, W.; Yan, Y.; Qu, J.; Liu, R. *Org. Biomol. Chem.* **2013**, *11*, 2254. (e) Sharma, D.; Sahoo, S. K.; Chaudhary, S.; Berac, R. K.; Callan, J. F. *Analyst* **2013**, *138*, 3646. (f) Wade, C. R.; Broomsgrove, A. E. J.; Aldridge, S.; Gabbaï, F. P. *Chem. Rev.* **2010**, *110*, 3958.

(22) Feng, D. J.; Li, X. Q.; Wang, X. Z.; Jiang, X. K.; Li, Z. T. *Tetrahedron* **2004**, *60*, 6137.

(23) Kosolapoff, G. M; Arpke, C. K.; Lamb, R. W.; Reich, H. J. *J. Chem. Soc.* **1968**, *7*, 815.

(24) *CrysAlisPRO*, Oxford Diffraction; Agilent Technologies UK Ltd: Yarnton, England, 2011.

(25) Farrugia, L. J. *WinGX*, Version 1.64.05; *J. Appl. Crystallogr.* **1999**, *32*, 837.

(26) Altomare, A.; Cascarano, G.; Giacovazzo, C.; Gualardi, A. *J. Appl. Crystallogr.* **1993**, *26*, 343.

(27) Sheldrick, G. M. *SHELXL-97*, Program for Structure Refinement; University of Göttingen: Germany, 1997.